The Rab Interacting Lysosomal Protein (RILP) Homology Domain Functions as a Novel Effector Domain for Small GTPase Rab36

Rab36 REGULATES RETROGRADE MELANOSOME TRANSPORT IN MELANOCYTES*[S]

Takahide Matsui[1], **Norihiko Ohbayashi**[1], and **Mitsunori Fukuda**[2]

From the Laboratory of Membrane Trafficking Mechanisms, Department of Developmental Biology and Neurosciences, Graduate School of Life Sciences, Tohoku University, Aobayama, Aoba-ku, Sendai, Miyagi 980-8578, Japan

Background: Rab36 is an uncharacterized small GTPase that is largely conserved in vertebrates.
Results: RILP family members and JIP3/4 contain a conserved RILP homology domain (RHD) that functions as an effector domain of Rab36.
Conclusion: RILP functions as a Rab36 effector that mediates retrograde melanosome transport in melanocytes.
Significance: Rab36 may regulate movements of Rab36-bearing vesicles/organelles through interaction with RHD-containing proteins.

Small GTPase Rab functions as a molecular switch that drives membrane trafficking through specific interaction with its effector molecule. Thus, identification of its specific effector domain is crucial to revealing the molecular mechanism that underlies Rab-mediated membrane trafficking. Because of the large numbers of Rab isoforms in higher eukaryotes, however, the effector domains of most of the vertebrate- or mammalian-specific Rabs have yet to be determined. In this study we screened for effector molecules of Rab36, a previously uncharacterized Rab isoform that is largely conserved in vertebrates, and we succeeded in identifying nine Rab36-binding proteins, including RILP (Rab interacting lysosomal protein) family members. Sequence comparison revealed that five of nine Rab36-binding proteins, *i.e.* RILP, RILP-L1, RILP-L2, and JIP3/4, contain a conserved coiled-coil domain. We identified the coiled-coil domain as a RILP homology domain (RHD) and characterized it as a common Rab36-binding site. Site-directed mutagenesis of the RHD of RILP revealed the different contributions by amino acids in the RHD to binding activity toward Rab7 and Rab36. Expression of RILP in melanocytes, but not expression of its Rab36 binding-deficient mutants, induced perinuclear aggregation of melanosomes, and this effect was clearly attenuated by knockdown of endogenous Rab36 protein. Moreover, knockdown of Rab36 in Rab27A-deficient melanocytes, which normally exhibit perinuclear melanosome aggregation because of increased retrograde melanosome transport activity, caused dispersion of melanosomes from the perinucleus to the cell periphery, but knockdown of Rab7 did not. Our findings indicated that Rab36 mediates retrograde melanosome transport in melanocytes through interaction with RILP.

Small GTPase Rab functions as a molecular switch that drives membrane trafficking by recruiting its specific effector molecules to specific membrane compartments (for review, see Refs. 1–3). The number of Rab isoforms varies from species to species, *e.g.* from 11 Rabs in budding yeasts to ~60 Rabs in mammals (4). The expansion of Rab isoforms in mammals is often regarded as being attributable to the acquisition of specialized membrane trafficking events in the specialized cell types of higher eukaryotes, but because of their large numbers, the precise function of most mammalian Rabs, especially of the mammalian-specific or vertebrate-specific Rabs, is largely unknown.

Rab36 is a previously uncharacterized Rab isoform that is mostly present in vertebrates. Although possible associations between Rab36 and human diseases, *e.g.* epilepsy, have recently been reported (5, 6), nothing is known about the function of endogenous Rab36 protein in membrane trafficking. The only information available has been that overexpression of a constitutive active mutant of Rab36 affects the spatial distribution of late endosomes and lysosomes (7). The most important step in learning the molecular mechanism of Rab36-mediated membrane trafficking is identifying its specific effector molecules (or its specific effector domains). Although several Rab36-binding proteins have recently been reported (7–9), whether they contain a common Rab36-binding site or whether they actually regulate Rab36-dependent membrane trafficking has never been investigated.

In this study we performed yeast two-hybrid screening for novel Rab36 effector molecules and identified nine Rab36-binding proteins, including seven novel ones. We also found that five of them, Rab interacting lysosomal protein (RILP),[3] RILP-L1 (RILP-like 1),

---

[S] This article contains supplemental Figs. S1–S6.
[1] Both authors contributed equally to this work.
[2] To whom correspondence should be addressed. Tel.: 81-22-795-7731; Fax: 81-22-795-7733; E-mail: nori@m.tohoku.ac.jp.

[3] The abbreviations used are: RILP, Rab interacting lysosomal protein; Appbp2, amyloid β precursor protein-binding protein 2; CC, coiled-coil; CA, constitutive active; CN, constitutive negative; EGFP, enhanced GFP; Ehbp1L1, EH domain binding protein 1-like 1; GAPCenA, GAP and centrosome-associated; Gripap1, GRIP1-associated protein 1; JIP3/4, JNK-interacting protein 3/4; Mreg, melano-regulin; mStr, monomeric strawberry; RHD, RILP homology domain; SR, shRNA-resistant; GTPγS, guanosine 5'-3-O-(thio)triphosphate.

RILP-L2, JIP3 (JNK-interacting protein 3), and JIP4, contain a conserved coiled-coil (CC) domain, and we identified the RILP homology domain (RHD) as a novel Rab36 binding domain. Site-directed mutagenesis revealed the residues in the RHD of RILP and in the switch II region of Rab36 are crucial for the Rab36-RILP interaction. We also discovered that Rab36 and its interaction with RILP are required for retrograde melanosome transport along microtubules in melanocytes. Based on these findings, we propose that Rab36 regulates movements of Rab36-bearing vesicles/organelles through interaction with the RHD-containing proteins.

EXPERIMENTAL PROCEDURES

Materials—Horseradish peroxidase (HRP)-conjugated anti-FLAG tag (M2) mouse monoclonal antibody and anti-FLAG tag antibody-conjugated agarose were obtained from Sigma. HRP-conjugated anti-T7 tag mouse monoclonal antibody and anti-T7 tag antibody-conjugated agarose were purchased from Merck. HRP-conjugated anti-HA tag mouse monoclonal antibody and anti-actin mouse monoclonal antibody were from Roche Applied Science and Applied Biological Materials (Richmond, BC, Canada), respectively. HRP-conjugated anti-red fluorescent protein antibody, HRP-conjugated anti-GFP (green fluorescent protein) antibody, and HRP-conjugated anti-GAPDH (3H12) mouse monoclonal antibody were from MBL (Nagoya, Japan). Anti-Rab7 rabbit polyclonal antibody and anti-Rab11 mouse monoclonal antibody were from Cell Signaling Technology (Danvers, MA) and BD Biosciences, respectively. Anti-melanoregulin rabbit polyclonal antibody and anti-RILP rabbit polyclonal antibody were prepared as described previously (10). Anti-Rab36 rabbit polyclonal antibody was produced by using purified glutathione *S*-transferase (GST)-mouse Rab36 (11) and affinity-purified as described previously (12). The specificity of the anti-Rab36 antibody was confirmed by using recombinant FLAG-tagged Rab7, Rab34, and Rab36 expressed in COS-7 cells (Fig. 6*A*). All other reagents used in this study were analytical grade or the highest grade commercially available.

Plasmid Construction and Ala-based Site-directed Mutagenesis—cDNAs encoding an open reading frame of the mouse Rab36-binding proteins, RILP-L2 (gene ID: 80291), Gripap1 (gene ID: 54645), Ehbp1L1 (gene ID: 114601), and Appbp2 (gene ID: 66884) were amplified from Marathon-Ready mouse whole brain and/or testis cDNAs (Clontech-Takara Bio Inc., Shiga, Japan) by PCR with specific pairs of oligonucleotides essentially as described previously (13). cDNAs of JIP3/mKIAA1066 and JIP4/mKIAA0516 were obtained from Dr. Takahiro Nagase (Kazusa DNA Research Institute, Chiba, Japan), and their open reading frame was similarly amplified by PCR. The sequences of the oligonucleotides used are available from the authors on request. Purified PCR products were directly inserted into the pGEM-T Easy vector (Promega, Madison, WI) and verified with an automated sequencer. The cDNAs were excised from the pGEM-T Easy vector with appropriate restriction enzymes and then subcloned into the pEF-T7 tag mammalian expression vectors modified from pEF-BOS as described previously (13, 14). The cDNAs of RILP, RILP-L1, and RILP-L2 were also subcloned into the pGAD-C1 vector

(15) and into the pEF-HA tag mammalian expression vectors (13, 16). pSilencer 2.1-U6 neo vector (Ambion, Austin, TX) expressing short hairpin RNA (shRNA) against Rab36 (named pSilencer-Rab36; 19-base target site, 5′-AGACTAGCCT-CATTCACAG-3′) was constructed as described previously (17). pEF-FLAG-Rab7, pEF-FLAG-Rab34, pEF-FLAG-Rab36, pEGFP-C1-Rab36, pmStr-C1-RILP, pEF-T7-GAPCenA, pSilencer-Rab7, pSilencer-RILP-st1, and pSilener-Mreg-st1 were prepared as described previously (10, 18 –20).

A Rab36 mutant carrying a Lys-to-Ala mutation at amino acid position 120 (K120A) or K120A/C121A mutations and RILP mutants (F222A, E226A, L231A, E233A, R234A, and N235A) were prepared by conventional PCR techniques with mutagenic oligonucleotides as described previously (21). An shRNA-resistant (SR) mutant of Rab36 was similarly prepared by PCR with a mutagenic oligonucleotide. The sequences of the mutagenic oligonucleotides used are also available from the authors on request. The mutant Rab36 fragments were subcloned into the pEF-FLAG tag vector (13) and pEGFP-C1 vector (Clontech-Takara Bio Inc.), and the mutant RILP fragments were subcloned into the pEF-T7 tag vector and pmStr-C1 vector (10).

Yeast Two-hybrid Assays—pGBD-C1-Rab36(Q116L)ΔCys (8) was used as bait to screen mouse testis and mouse embryo mixed cDNA libraries (oligo(dT)-primed) according to the manufacturer's instructions (Clontech-Takara Bio Inc.), and ~1 × 10⁸ colonies were investigated. After DNA sequencing and data base searching, the Rab binding specificity of positive clones was further investigated by using a panel of 60 different constitutive active/negative (CA/CN) mutants of Rabs lacking a C-terminal geranylgeranylation site essentially as described previously (8, 22, 23). The clones that we used to determine Rab binding specificity are indicated by *solid lines* in Fig. 1. Because RILP family members are relatively small proteins, full-length constructs were also used to determine Rab binding specificity, and they yielded the same results as in the short clones obtained by the two-hybrid screening. The yeast strain, medium, culture conditions, and transformation protocol are described in James *et al.* (15). The materials used for the two-hybrid assay in this study were: yeast strain pJ69 – 4A, pGAD-C1, or pAct2 plasmid (Clontech-Takara Bio Inc.) for expression of the activating domain fusion protein, pGBD-C1 plasmid for expression of the DNA binding domain fusion protein, a synthetic complete medium lacking leucine and tryptophan (SC-LW medium; 0.67% yeast nitrogen base without amino acids, 2% glucose, 2% Bacto agar, 0.02% adenine, 0.01% uracil, 0.01% histidine, 0.015% lysine, and 0.01% methionine), and a synthetic complete medium lacking adenine, histidine, leucine, and tryptophan (SC-AHLW medium) as the selection medium.

Sequence Analyses—Multiple sequence alignment of the Rab36 binding domain of RILP, RILP-L1, RILP-L2, JIP3, and JIP4 was performed by using the ClustalW program (version 1.83) set at the default parameters. The domain structures of the Rab36-binding proteins identified in this study were analyzed with the Simple Modular Architecture Research Tool (SMART) program and the Coils program using the MTIDK matrix with 2.5-hold weighting of positions a and d (Version 2.2). Sequence alignment of the switch II region of mouse or
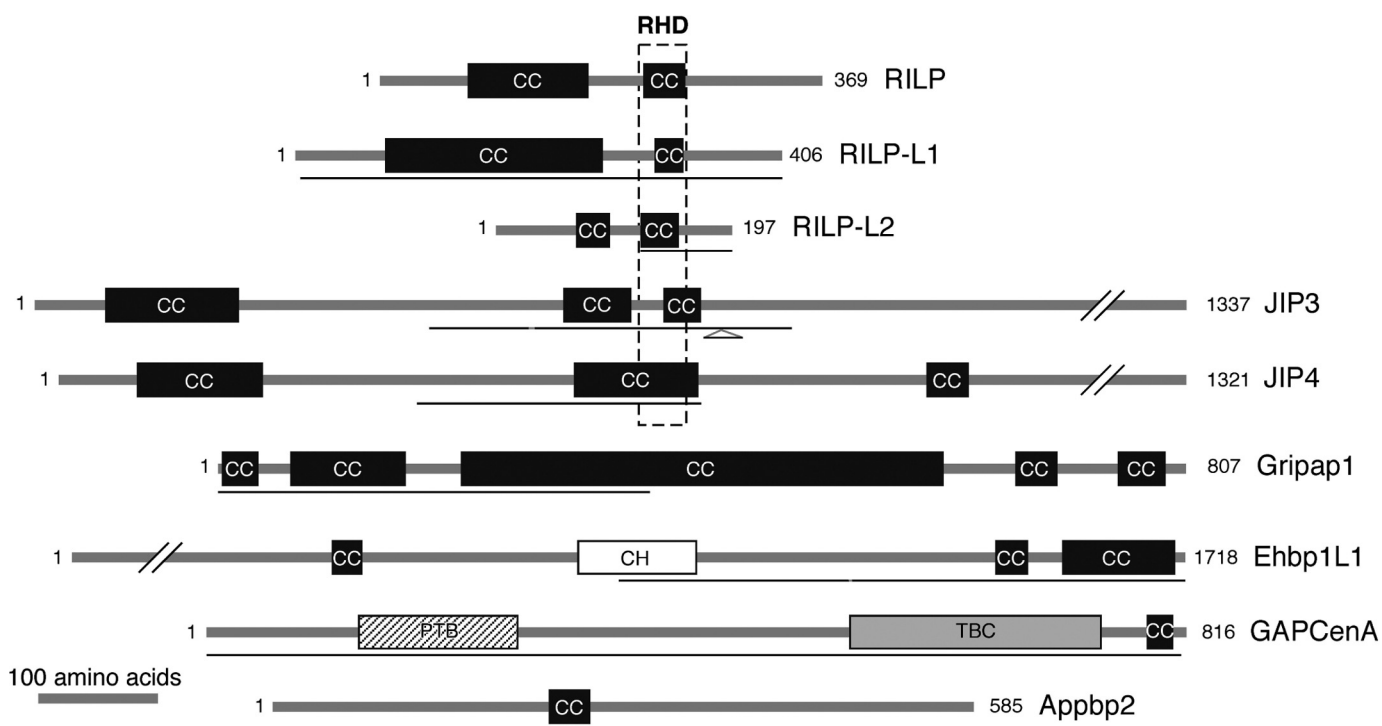
FIGURE 1. **Schematic representation of mouse Rab36-binding proteins identified in this study.** Amino acid numbers are shown on both sides. *Solid lines* indicate the constructs obtained by the yeast two-hybrid assays (see Fig. 2). The JIP3 construct and Ehbp1L1 construct contain a small deletion (*gray region on the solid lines*), and the JIP3 construct also contains an insertion. The domain structures of the Rab36-binding proteins identified were analyzed with the SMART program or Coils program (for Appbp2) as described under "Experimental Procedures." A homology search analysis revealed the presence of a conserved region (referred to as the RILP homology domain, RHD) in RILP, RILP-L1, RILP-L2, JIP3, and JIP4. *CC,* coiled-coil domain (*black boxes*); *CH,* calponin homology domain (*open box*); *PTB,* phosphotyrosine binding domain (*hatched box*); *TBC,* Tre-2/Bub2/Cdc16 (*shaded box*).

human Rabs was performed by using the GENETYX-MAC software program (Version 15.0.1; GENETYX Corp., Tokyo, Japan).

Cell Cultures and Transfections—The immortal mouse melanocyte cell lines melan-a, derived from a black mouse, and melan-ash, derived from an *ashen* mouse, both generous gifts of Dorothy C. Bennett (St George's Hospital Medical School, London, UK), were cultured on glass-bottom dishes (35-mm dish; MatTek, Ashland, MA) (24–26). Plasmids were transfected into melanocytes by using FuGENE 6 (Roche Applied Science) according to the manufacturer's instructions. Two days after transfection, cells were fixed in 4% paraformaldehyde and examined for fluorescence with a confocal fluorescence microscope (Fluoview; Olympus, Tokyo, Japan), and the images were processed with Adobe Photoshop software (CS4). For immunostaining of RILP, *RILP* shRNA-transfected melan-a cells were fixed in 4% paraformaldehyde, permeabilized with 0.3% Triton X-100, and stained with anti-RILP rabbit antibody (6.9 μg/ml) as described previously (10). The RILP antibody was visualized with anti-rabbit Alexa Fluor 594-conjugated IgG (Invitrogen) and examined for fluorescence with a confocal fluorescence microscope as described above. Melanosome distribution assays (*i.e.* perinuclear aggregation *versus* peripheral distribution) were performed as described previously ($n > 50$ from three independent dishes) (26), and the data are expressed as the means and S.E. Statistical analyses were performed by Student's unpaired *t* test.

Immunoaffinity Purification of Mature Melanosomes—Immunoaffinity purification of melanosomes with anti-tyrosinase IgG-conjugated magnetic beads was performed essentially as described previously (17). In brief, melan-a cells (one 10-cm dish of confluent cells) were homogenized in a homogenization buffer (5 mM HEPES-KOH, pH7.2, 5 mM EGTA, 0.03 M sucrose, and appropriate protease inhibitors). After centrifugation at $800 \times g$ for 10 min, the supernatant obtained was incubated for 2 h at 4 °C with anti-tyrosinase rabbit polyclonal antibody or control rabbit IgG coupled with Dynabeads M-280 (Invitrogen) in the presence of 1% bovine serum albumin. After washing the beads twice with PBS, the bound fractions were subjected to 10% SDS-PAGE followed by immunoblotting with the antibodies against Rab36 and a variety of organelle markers as described previously (10).

Miscellaneous Procedures—*In vitro* binding experiments between two proteins, *e.g.*, between HA-RILP and FLAG-Rab36, in COS-7 cells, direct binding experiments between purified GST-Rab36 and T7-RILP/T7-RILP-L1/T7-RILP-L2, SDS-PAGE, and immunoblotting were performed as described previously (13, 27).

RESULTS

Identification of Novel Rab36-binding Proteins by Yeast Two-hybrid Screening—We performed yeast-two hybrid assays with a GTP-locked, constitutive active mutant of Rab36 as bait, and we obtained eight different positive clones. Sequence analysis revealed them to be RILP-L1, RILP-L2, JIP3, JIP4, Gripap1 (GRIP1-associated protein 1), Ehbp1L1 (EH domain binding protein 1-like 1), GAPCenA (GAP and centrosome-associated), and Appbp2 (amyloid β precursor
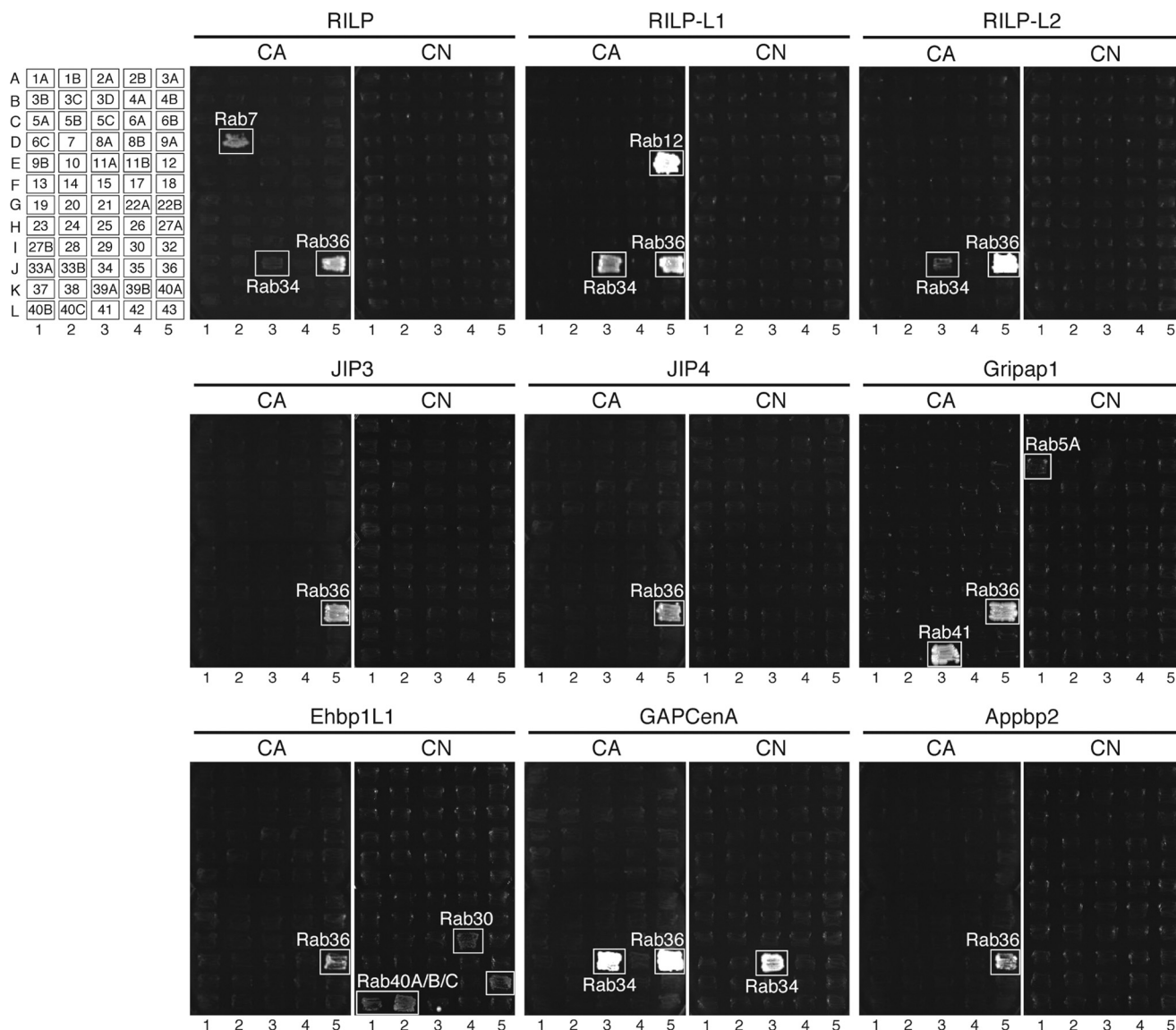
FIGURE 2. **Rab binding specificity of the Rab36-binding proteins identified in this study.** Rab binding activity of mouse RILP, RILP-L1, and RILP-L2 (*top row*); JIP3, JIP4, and Gripap1 (*middle row*); Ehbp1L1, GAPCenA, and Appbp2 (*bottom row*). Yeast cells containing pGBD plasmid expressing a constitutive active form (CA, which mimics the GTP-bound form) (8, 19) or a constitutive negative form (CN, which mimics the GDP-bound form) (22, 23) of Rab (positions are indicated in the *left panels*) and pGAD plasmid expressing the full-length RILP, RILP-L1, or RILP-L2 or pAct2 plasmid expressing the fragment of JIP3, JIP4, Gripap1, Ehbp1L1, GAPCenA, or Appbp2 (see *solid lines* in Fig. 1). The yeast cells expressing the Rab36-binding proteins indicated were streaked on SC-AHLW medium and incubated at 30 °C for 1 week. Positive patches are *boxed*. Note that JIP3, JIP4, and Appbp2 specifically recognized the CA form of Rab36, whereas the other Rab36-binding proteins also bound the CA and/or CN form of Rabs other than Rab36.

protein-binding protein 2) (Fig. 1). Interaction between GAPCenA and Rab36 had already been demonstrated by GST pulldown assays (9), but the others are novel Rab36-binding proteins. Protein motif analysis indicated that all of these proteins contained one or more CC domains, which often function as Rab binding domains (8), suggesting that these Rab36-binding proteins might contain a common Rab36-binding site. To investigate this possibility, the ClustalW program was used to perform a detailed sequence comparison between them, with particular focus on the CC domains. As expected, four Rab36-binding proteins, RILP-L1, RILP-L2, JIP3, and JIP4, were found to contain conserved CC domains. By contrast, none of the CC domains of Gripap1, Ehbp1L1, GAPCenA, and Appbp2 showed any clear sequence homology with each other. Moreover, data base searching revealed the

presence of a similar conserved CC domain (~40 amino acids) in RILP that has recently been shown to bind Rab36 *in vitro* (7). We, therefore, named this conserved region in RILP, RILP-L1, RILP-L2, JIP3, and JIP4 the RILP homology domain (RHD; *dotted box* in Fig. 1).

Because RILP was originally identified as a Rab7 effector (28, 29), it was thought that the RHD might primarily function as a Rab7 binding domain rather than as a Rab36 binding domain. To rule out this possibility, we compared the Rab binding specificity of RILP, RILP-L1, RILP-L2, JIP3, and JIP4 by yeast two-hybrid assays with the panel of 60 different Rab CA/CN mutants (Fig. 2). As expected, none of them except RILP bound Rab7, and all of them bound the CA form of Rab36 but not its CN form. It should be noted that both JIP3 and JIP4 specifically bound Rab36. By contrast, RILP, RILP-L1, and RILP-L2 each

bound several Rabs, *i.e.* Rab7/34/36, Rab12/34/36, and Rab34/36, respectively, and their Rab36 binding activity appeared to be the strongest (*i.e.* the growth rate of yeast cells expressing Rab36 was relatively fast). These results indicated that the RHD of the RILP family members and JIP3/4 is likely to function as an effector domain for Rab36.

We also determined the Rab binding specificity of Gripap1, Ehbp1L1, GAPCenA, and Appbp2 (Fig. 2). In contrast to the RHD described above, however, Gripap1, Ehbp1L1, and GAPCenA bound a CN form of several Rabs and exhibited different Rab binding specificity. For example, Gripap1 bound Rab36(CA), Rab41(CA), and Rab5A(CN), and Ehbp1L1 bound Rab36(CA), Rab30(CN), and Rab40(CN). Because no clear sequence homology was found between Gripap1, Ehbp1L1, GAPCenA, and Appbp2, each of these proteins may have a unique Rab36 binding domain. We, therefore, focused on the RHD as a candidate Rab36 effector domain and attempted to characterize the RHD of three members of the RILP family, RILP, RILP-L1, and RILP-L2, in greater detail.

GTP-dependent and Direct Interaction of RILP with Rab36— To determine whether the interaction between the full-length RILP family members and Rab36 occurs in mammalian cultured cells, co-immunoprecipitation assays in COS-7 cells were performed in the presence of 0.5 mM GTPγS (or 1 mM GDP) as described previously (13, 27). Consistent with the results of the yeast two-hybrid assays (Fig. 2), RILP bound Rab36 more preferably in the presence of GTPγS than in the presence of GDP (Fig. 3*A*, *right panels*). Similarly, RILP also bound Rab7 in a GTP-dependent manner (28, 29), whereas neither RILP-L1 nor RILP-L2 bound Rab7 even in the presence of GTPγS (Fig. 3*A*, *left panels*). Direct interaction between the RILP family members and Rab36 was further investigated by using purified components, *i.e.* T7-RILP and GST-Rab36. As expected, T7-RILP (T7-RILP-L1 or T7-RILP-L2) directly bound GST-Rab36 (Fig. 3*B*, *lanes 6*, *8*, and *10*), but not GST alone. We, therefore, concluded that the RILP family members are GTP-dependent and direct binding partners of Rab36 in mammalian cells.

Identification of the Critical Residues Responsible for Rab36 Binding of RILP— To identify the structural determinants of the RHD-Rab36 interaction, we first compared the amino acid sequence of the five RHDs (Fig. 4*A*), and the results showed that six amino acids, Phe-222, Glu-226, Leu-231, Glu-233, Arg-234, and Asn-235, were conserved in all of the RHDs (*asterisks* in Fig. 4*A*). We considered these residues to be candidates for the residues that specifically recognize Rab36, and we, therefore, performed an Ala-based site-directed mutagenesis (*arrowheads* in Fig. 4*A*). As shown in Fig. 4*B*, these residues contributed differently to the recognition of Rab7, Rab34, and Rab36. Neither the RILP(L231A) mutant nor the RILP(R234A) mutant bound Rab7, Rab34, or Rab36 at all, indicating that Leu-231 and Arg-234 are required for Rab7/34/36 binding. Glu-226 and Asn-235, on the other hand, are required for Rab34 binding, and Glu-233 is required for Rab7/34 binding.

We then performed co-immunoprecipitation assays in COS-7 cells to validate the effect of these mutations on Rab36 binding in mammalian cells. Consistent with the results of the
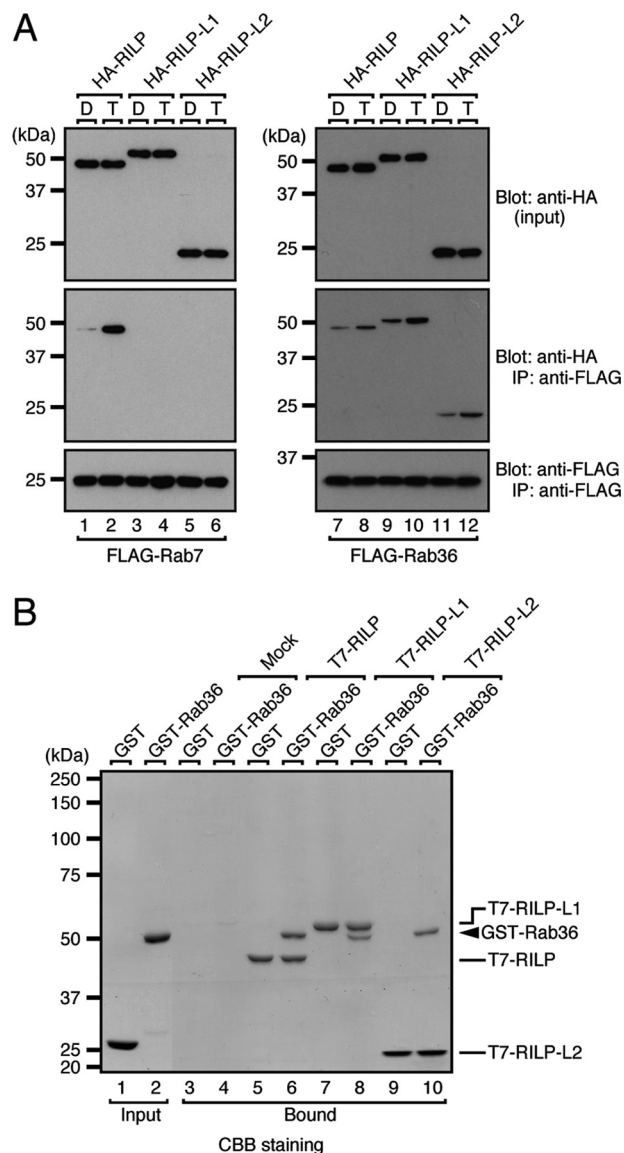

FIGURE 3. Rab36 binding activity of the RILP family members. *A*, GTP-dependent interaction between the RILP family members and Rab7 or Rab36 is shown. The association between HA-tagged RILP/RILP-L1/RILP-L2 and FLAG-tagged Rabs in COS-7 cell lysates was evaluated by co-immunoprecipitation assays with anti-FLAG tag antibody-conjugated agarose beads as described previously (13, 27). Co-immunoprecipitated HA-RILP/RILP-L1/RILP-L2 (*middle panels*) and immunoprecipitated (*IP*) FLAG-Rab7/36 (*bottom panels*) were detected with HRP-conjugated anti-HA tag antibody and HRP-conjugated anti-FLAG tag antibody, respectively. Under our experimental conditions, RILP appears to preferentially bind Rab7 rather than Rab36. Input means 1/80 volume of the reaction mixture used for immunoprecipitation (*top panels*). *B*, shown is direct interaction between the RILP family members and Rab36. Agarose beads coupled with purified T7-RILP/RILP-L1/RILP-L2 were incubated with GST-Rab36 or GST alone as a control. Proteins bound to the beads were detected with Coomassie Brilliant Blue R-250 (*CBB*) staining (*lanes 3–10*). *Input* means 1/80 volume of the reaction mixture used for the binding assay (*lanes 1* and *2*). The positions of the molecular mass markers (in kilodaltons) are shown on the *left*.

yeast two-hybrid assays (Fig. 4*B*), neither the RILP(L231A) mutant nor the R234A mutant exhibited Rab36 binding activity, whereas both the RILP(E233A) mutant and the RILP(N235A) mutant bound Rab36, the same as the wild-type protein, despite the loss of Rab7/34 binding activity and Rab34 binding activity, respectively (Fig. 4*C*).
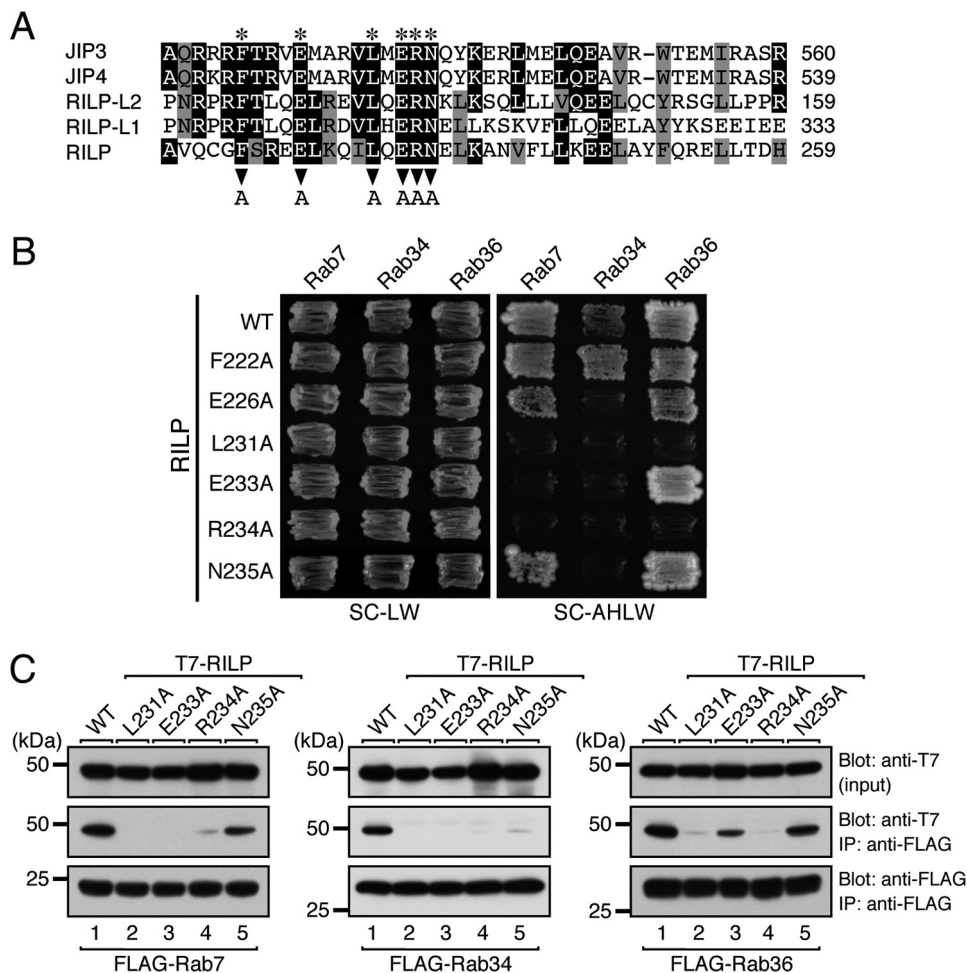
FIGURE 4. **Identification of critical residues responsible for Rab36 binding in the RHD of RILP by site-directed mutagenesis.** *A*, shown is sequence alignment of the RHD of mouse RILP, RILP-L1, RILP-L2, JIP3, and JIP4. Identical residues and residues conserved in more than three of the sequences are shown against a *black background* and a *gray background*, respectively. The *asterisks* indicate the positions of six highly conserved amino acids in the RHD that were the focus of the Ala-based site-directed mutagenesis (*arrowheads*). *B*, yeast two-hybrid assays revealed that the Leu-231 and Arg-234 of RILP in the RHD are critical for Rab7/34/36 binding. Yeast cells containing the pGAD plasmid expressing one of the RILP mutants indicated and pGBD plasmid expressing one of the Rab(CA) mutants indicated were streaked on SC-LW (*left panel*) and SC-AHLW (selection medium; *right panel*) and incubated at 30 °C for 1 day and 1 week, respectively. Note that Glu-226 and Asn-235 are required for Rab34 binding, Glu-233 is required for both Rab7 binding and Rab34 binding, and Leu-231 and Arg-234 is required for binding of all three Rabs. *C*, Rab binding activity of RILP mutants is shown. Associations between T7-tagged RILP wild-type (*WT*) or mutants and FLAG-tagged Rab7, Rab34, or Rab36 in the presence of 0.5 mM GTPγS were analyzed by co-immunoprecipitation assays with anti-FLAG tag antibody-conjugated agarose beads as described previously (13, 27). Co-immunoprecipitated T7-RILP (*middle panels*) and immunoprecipitated FLAG-Rabs (*IP*; *bottom panels*) were detected with the antibodies indicated. *input* means 1/80 volume of the reaction mixture used for immunoprecipitation (*top panels*). The positions of the molecular mass markers (in kilodaltons) are shown on the *left*.

Identification of the Critical Residues Responsible for RILP Binding of Rab36—Next, we attempted to identify the critical residues that are responsible for RILP binding of Rab36. To do so, we focused on the switch II sequence of Rab36, because the switch II region of other Rabs has been shown to be required for the specific recognition of effector molecules, *e.g.* the Rab3-rabphilin interaction (30), Rab27-Slac2-a interaction (16, 31), and Rab32/38-Varp interaction (32). Sequence comparison of the switch II region of 60 different Rabs indicated that the Lys-120 and Cys-121 of Rab36 are conserved only in Rab36 and Rab34 (supplemental Fig. S1, *red background*), the most closely related isoform of Rab36 in the phylogenetic tree (33) that also binds RILP (Fig. 2) (29). Involvement of these residues in RILP binding was also evaluated by Ala-based site-directed mutagenesis combined with yeast two-hybrid assays (Fig. 5A, *arrowheads*). As shown in Fig. 5B, both Rab36(K120A) and

Rab36(K120A/C121A) clearly exhibited weaker RILP binding activity than the wild-type Rab36. Essentially the same results were obtained by co-immunoprecipitation assays in COS-7 cells (Fig. 5C). The Rab36(K120A/C121A) mutant hardly interacted with RILP at all, whereas the wild-type Rab36 strongly interacted with RILP.

Involvement of Rab36 Together with RILP in Retrograde Melanosome Transport in Melanocytes—In the final set of experiments we sought to determine whether Rab36 actually functions together with RILP in a particular membrane trafficking pathway. To do so, we first investigated the profile of Rab36 protein expression in a variety of mouse tissues and cell lines by immunoblotting with an isoform-specific antibody (Fig. 6A). In contrast to the ubiquitous and abundant expression of Rab11, Rab36 was found to exhibit restricted expression patterns in mouse tissues and cell lines, *e.g.* mouse testis, brain, melan-a
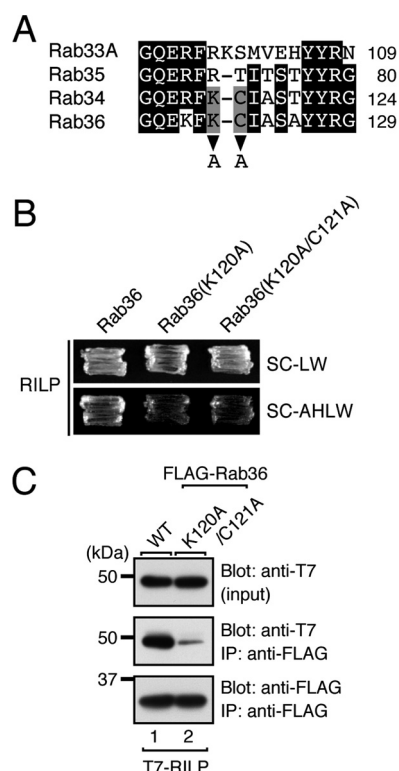
A

Rab33A GQERF RKSMVEHYYRN 109
Rab35 GQERF R-TTSTYYRG 80
Rab34 GQERF K-CIASTYYRG 124
Rab36 GQEKF K-CIASAYYRG 129
A A

B

C

FIGURE 5. **Identification of critical residues responsible for RILP binding in the switch II region of Rab36 by site-directed mutagenesis.** *A*, shown is the sequence alignment of the switch II region of mouse Rab33A, Rab34, Rab35, and Rab36. Identical residues are shown against a b*lack background*. Two highly conserved amino acids in the switch II region of Rab34 and Rab36 are shown against a *gray background* (see also supplemental Fig. S1). The *arrowheads* indicate the positions that were the focus of the Ala-based site-directed mutagenesis. *B*, yeast two-hybrid assays revealed that the Lys-120 and Cys-121 of Rab36 are critical for RILP binding. Yeast cells containing the pGAD plasmid expressing RILP and pGBD plasmid expressing one of the Rab(CA) mutants indicated were streaked on SC-LW (*upper panel*) and SC-AHLW (selection medium; *lower panel*) and incubated at 30 °C for 1 and 2 days, respectively. *C*, shown is RILP binding activity of the Rab36(K120A/C121A) mutant. Associations between T7-tagged RILP and FLAG-tagged Rab36 in the presence of 0.5 mM GTPγS were analyzed by co-immunoprecipitation assays with anti-FLAG tag antibody-conjugated agarose beads as described previously (13, 27). Co-immunoprecipitated T7-RILP (*middle panel*) and immunoprecipitated (IP) FLAG-Rab (*bottom panel*) were detected with the antibodies indicated. *Input* means 1/80 volume of the reaction mixture used for immunoprecipitation (*top panel*). The positions of the molecular mass markers (in kilodaltons) are shown on the *left*.

A

B

C

FIGURE 6. **Expression of Rab36 protein in mouse tissues and in a variety of cell lines.** *A*, the specificity of the anti-Rab36 antibody is shown. Total cell lysates expressing either FLAG-tagged Rab7, Rab34, or Rab36 were analyzed by 10% SDS-PAGE followed by immunoblotting with anti-Rab36 antibody (1 μg/ml) and HRP-conjugated anti-FLAG tag antibody (1/10,000 dilution). Note that anti-Rab36 antibody specifically recognized Rab36 (lane 3) but did not recognize Rab7 (*lane 1*) or Rab34, a closely related isoform of Rab36 (*lane 2*). *B*, restricted expression patterns of Rab36 protein in mouse tissues are shown. Tissue homogenates (25 μg each) of mouse brain, heart, lung, liver, kidney, spleen, and testis were analyzed by immunoblotting with anti-Rab36 antibody (1 μg/ml, *upper panels*) and anti-Rab11 antibody (1/200 dilution, *lower panels*). Note that Rab36 was expressed abundantly in the testis, moderately in the brain, and very weakly in the other tissues. The higher immunoreactive band in the mouse liver presumably corresponds to a nonspecific band or a post-translational modified form of Rab36 protein (*asterisk*). *C*, restricted expression of Rab36 protein in mouse, rat, or human cell lines is shown. Total lysates of the cells indicated were analyzed by immunoblotting with anti-Rab36 antibody (1 μg/ml, *upper panel*) and anti-GAPDH antibody (1/10,000 dilution, *lower panel*). Note that abundant expression of Rab36 protein was found in mouse testis, melan-a cells (melanocytes), and PC12 cells (neuroendocrine cells). The positions of the molecular mass markers (in kilodaltons) are shown on the *left*.

cells, and PC12 cells expressed Rab36, but mouse embryonic fibroblast cells and HeLa-S3 cells did not (Fig. 6, *B* and *C*). We especially focused on one of the Rab36-expressing cell lines, melan-a cells (a melanocyte cell line derived from a black mouse) (24), because melan-a cells also endogenously express RILP (10). Because we previously showed that overexpression of RILP in melan-a cells often induced perinuclear melanosome aggregation by promoting microtubule-based retrograde melanosome transport (10), we next investigated whether Rab36 is also involved in this process. When enhanced green fluorescent protein (EGFP)-tagged Rab36 was expressed in melan-a cells, ~50% of the Rab36-expressing cells exhibited perinuclear melanosome aggregation (Fig. 7, *C* and *D*) the same as the monomeric strawberry (mStr)-tagged RILP-expressing cells had (Fig. 7, *A* and *B*). When EGFP-Rab36 alone was expressed in melan-a cells, most of it was located around the perinuclear region (presumably the Golgi) (7) (Fig. 7*C*), whereas when
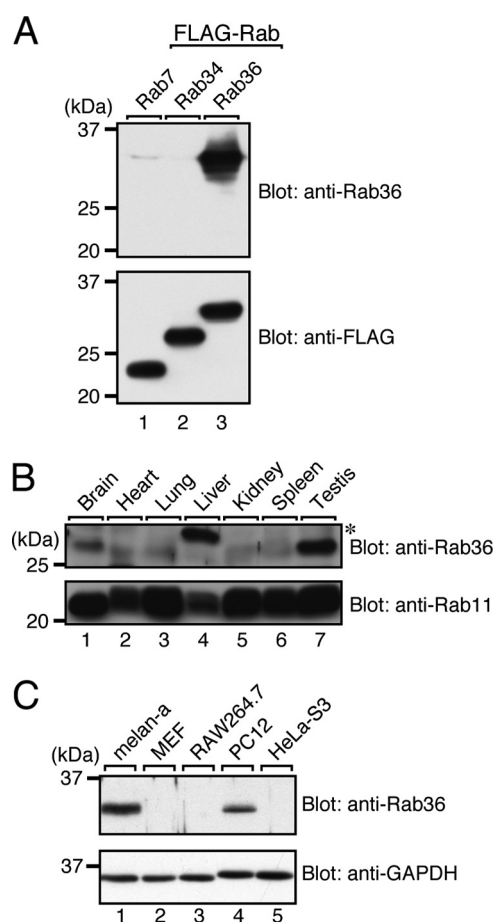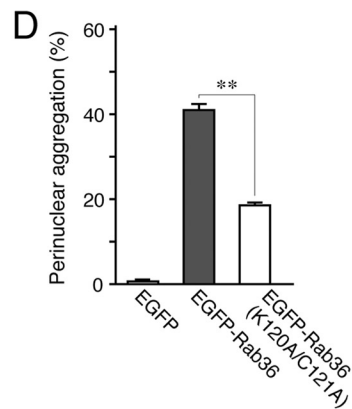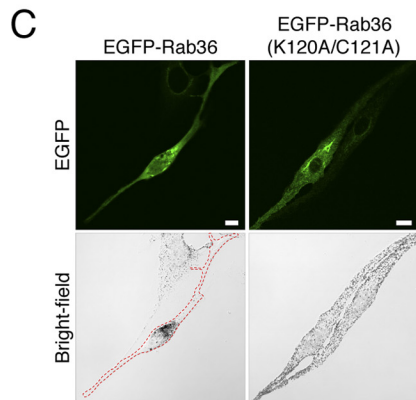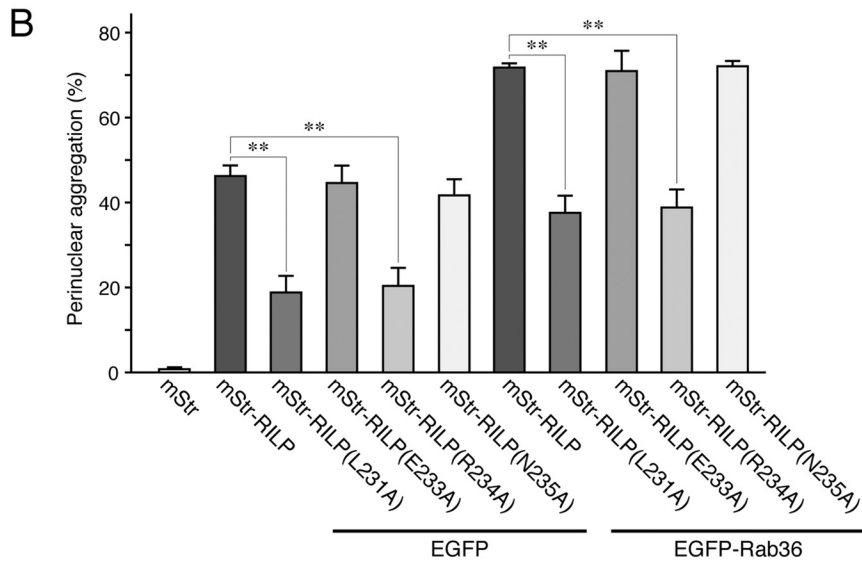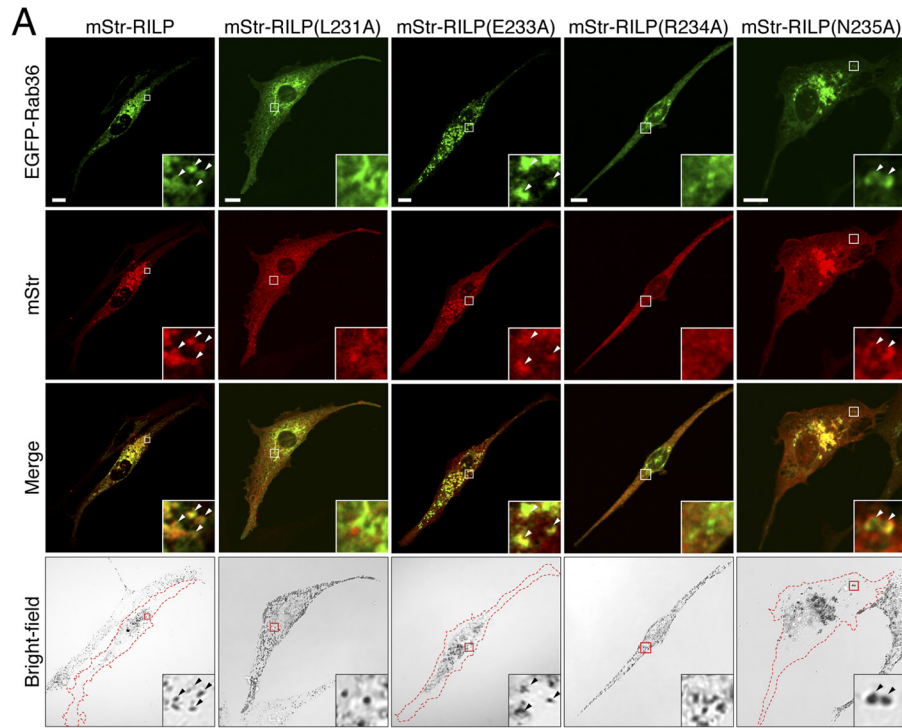
EGFP-Rab36 and mStr-RILP were co-expressed in melan-a cells, they were often found on mature melanosomes (Fig. 7*A*, *insets* in the *far left panels*). The presence of endogenous Rab36 protein on mature melanosomes and the presence of RILP protein on mature melanosomes were confirmed by immunoaffinity purification of mature melanosomes (supplemental Fig. S2*A*) and by immunofluorescence analysis (supplemental Fig. S2*B*), respectively.

To determine whether Rab36 actually functions together with RILP, we evaluated the effect of different RILP mutants with different Rab binding specificities (Fig. 4*B*) on the distri-

bution of melanosomes in melan-a cells. Interestingly, both the RILP(E233A) mutant, which binds Rab36 alone, and the RILP(N235A) mutant, which binds both Rab7 and Rab36, behaved in the same way as the wild-type RILP (Fig. 7B). By contrast, two Rab36 binding-deficient mutants, RILP(L231A) and RILP(R234A), did not efficiently induce perinuclear melanosome aggregation (~20% of the transfected cells exhibited the aggregation phenotype; **, $p < 0.01$, in comparison with the cells that expressed the wild-type RILP) (Fig. 7B). Rab36-dependent perinuclear melanosome aggregation was much more evident when both Rab36 and RILP (wild-type or mutants) were co-expressed in melan-a cells (Fig. 7, *A* and *B*). Expression of both Rab36 and wild-type RILP additively increased the proportion of cells that exhibited the melanosome aggregation phenotype (more than 70% of the transfected cells). Co-expression of Rab36 with the Rab36 binding RILP mutant RILP(E233A) or RILP(N235A) also efficiently induced perinuclear melanosome aggregation, whereas the Rab36 binding-deficient mutants RILP(L231A) and RILP(R234A) did not exhibit any additive effect even when co-expressed with Rab36 (~40% of the transfected cells exhibited the aggregation phenotype). These results clearly indicated that the perinuclear melanosome aggregation phenotype induced by RILP is entirely dependent on its Rab36 binding ability and that it is not dependent on its Rab7 binding ability or Rab34 binding ability.

If Rab36 actually induces perinuclear melanosome aggregation through a direct interaction with RILP (Fig. 3B), a Rab36 mutant (K120A/C121A) with reduced RILP binding activity should not efficiently induce the perinuclear melanosome aggregation phenotype. As expected, expression of Rab36(K120A/C121A) in melan-a cells induced perinuclear melanosome aggregation less effectively than the wild-type Rab36 did (Fig. 7, *C* and *D*). Taken together the results of the mutational analyses of RILP and Rab36 described above indicated that formation of the RILP-Rab36 complex mediates perinuclear melanosome aggregation in melanocytes. Consistent with these results, RILP-induced perinuclear melanosome aggregation was clearly suppressed by knockdown of endogenous Rab36 protein, although RILP still had the ability to induce perinuclear melanosome aggregation even in Rab36-deficient cells (Fig. 8, *A* and *B*). We hypothesized that its residual activity is mediated by melanoregulin (Mreg, a dilute suppressor (*dsu*) gene product), another RILP-binding protein recently identified as a cargo receptor for retrograde melanosome transport (10), and consistent with our hypothesis, dou-

ble knockdown of Rab36 and Mreg by specific shRNAs inhibited the perinuclear melanosome aggregation induced by RILP much more strongly than knockdown of either Rab36 or Mreg alone (Fig. 8).

To directly determine whether endogenous Rab36 protein is actually involved in retrograde melanosome transport, we conducted knockdown experiments on melan-ash cells, which normally exhibit perinuclear melanosome aggregation due to increased retrograde melanosome transport activity (25), because we had previously shown that functional disruption of the retrograde melanosome transport complex in melan-a cells has no effect on peripheral melanosome distribution (10). In contrast to the results of the overexpression study, knockdown of endogenous Rab36 protein by the specific shRNA restored peripheral melanosome distribution, *i.e.* dispersion of melanosomes from the perinucleus to the cell periphery (Fig. 9, *A* and *B*), the same as RILP knockdown had done as described previously (10), whereas consistent with our previous report (10), knockdown of Rab7 had no effect on perinuclear melanosome aggregation. The effect of Rab36 knockdown in melan-ash cells cannot have been attributable to an off-target effect of the shRNA used, because re-expression of an SR form of Rab36 in Rab36-deficient melan-ash cells restored the perinuclear melanosome aggregation phenotype (Fig. 9, *A* and *B*). It should be noted that the mutant Rab36^{SR}(K120A/C121A), which exhibited reduced RILP binding activity (Fig. 5), was unable to restore perinuclear melanosome aggregation. These results allowed us to conclude that Rab36 regulates retrograde melanosome transport in melanocytes through interaction with RILP.

DISCUSSION

In this study we identified nine putative Rab36 effector proteins, including seven novel ones, by yeast two-hybrid screening and identified the RHD as a novel GTP-dependent Rab36 binding domain (Figs. 2 and 3). However, the Rab binding specificity of the RHDs differs slightly among the RILP family members and JIP3/4: RILP interacts with Rab7, Rab34, and Rab36; RILP-L1 interacts with Rab12, Rab34, and Rab36; RILP-L2 interacts with Rab34 and Rab36; JIP3/4 interacts with Rab36 alone. Although RILP has been extensively characterized as a Rab7 effector that regulates lysosomal trafficking in various cell lines (28, 29, 34, 35), phagosome maturation in RAW264.7 cells (36), and lytic granule movement in cytotoxic T-lymphocytes (37), our results clearly indicated that RILP regulates retrograde melanosome transport in melanocytes through interaction

FIGURE 7. **Effect of expression of RILP mutants or a Rab36 mutant on melanosome distribution in melan-a cells.** *A*, expression of Rab36-binding mStr-RILP mutants, but not of Rab36-binding-deficient mStr-RILP mutants, together with EGFP-Rab36 in melan-a cells efficiently induced perinuclear melanosome aggregation. Typical images of mStr-RILP (WT or mutants)- and EGFP-Rab36-expressing cells and their corresponding bright-field images are shown (low magnification views of typical bright-field images are also shown in supplemental Fig. S5). mStr-RILP (WT, E233A, or N235A)- and EGFP-Rab36-expressing cells with perinuclear melanosome aggregation are *outlined with a broken red line*. The *insets* show magnified views of the boxed areas. *Arrowheads* indicate colocalization between Rab36, RILP, and melanosomes. Note that RILP mutants that failed to form the Rab36-RILP complex did not efficiently induce perinuclear melanosome aggregation. The level of protein expression of mStr-RILP mutants is shown in supplemental Fig. S6A. *Scale bars*, 10 μm. *B*, the number of melanocytes showing perinuclear melanosome aggregation is expressed as a percentage of the number of transfected melanocytes shown in *A*. **, $p < 0.01$ by Student's unpaired *t* test. *C*, expression of WT Rab36, but not a K120A/C121A mutant, in melan-a cells efficiently induced perinuclear melanosome aggregation. EGFP-Rab36 (WT or K120A/C121A) was transfected into melan-a cells. Typical images of EGFP-Rab36 (WT or K120A/C121A)-expressing cells and their corresponding bright-field images are shown. EGFP-Rab36-expressing cells with perinuclear melanosome aggregation are *outlined with a broken red line*. Note that the Rab36(K120A/C121A) mutant that failed to form the stable Rab36-RILP complex did not efficiently induce perinuclear melanosome aggregation. The level of protein expression of EGFP-Rab36 (WT and K120A/C121A mutant) is shown in supplemental Fig. S6B. *Scale bars*, 10 μm. *D*, the number of melanocytes showing perinuclear melanosome aggregation is expressed as a percentage of the number of transfected melanocytes shown in *C*. **, $p < 0.01$ by Student's unpaired *t* test.

with Rab36 and not with Rab7 (Figs. 7–9). Because RILP also interacts with Mreg, which regulates retrograde melanosome transport, and the Mreg-binding site overlaps the Rab-binding site (10), Rab36 and Mreg are likely to function as independent cargo receptors for a dynein-dynactin motor complex. Actually, the knockdown effects of Rab36 and of Mreg were additive (Fig. 8). Our findings in regard to the two cargo receptors explain the reason for the discrepancy between our recent report that knockdown of Mreg in melan-ash cells restored peripheral melanosome distribution and a previous report that *dsu/dilute* double mutant (Mreg- and myosin Va-deficient) did not reverse the *dilute* phenotype of perinuclear melanosome aggregation (38). Rab36 presumably functions as an alternate cargo receptor for retrograde melanosome transport in *dsu/dilute* double mutant mice.

The results of the site-directed mutagenesis of RILP indicated that Leu-231 and Arg-234, both of which are conserved in all of the RHDs, are crucial for Rab36 binding activity (Fig. 4). These residues presumably contribute to recognition of the specific sequence (*e.g.* Lys-120 and Cys-121; supplemental Fig. S1) of the switch II region of Rab36, *i.e.* an effector interaction site. Actually, a switch II mutant of Rab36(K120A/C121A) exhibited dramatically less binding activity toward all of the RHD-containing proteins except RILP-L1 (Fig. 5 and supplemental Fig. S3). Interestingly, however, the Rab36(K120A/C121A) mutant bound other non-RHD Rab36-binding proteins (Gripap1, GAPCenA, Ehbp1L1, and Appbp2; supplemental Fig. S3) normally, suggesting that their Rab36 recognition mechanisms differ from that of the RHD. Because interaction between Rab36 and the full-length Gripap1, GAPCenA, and Appbp2, but not with the full-length Ehbp1L1, was observed in mammalian cultured cells (supplemental Fig. S4), these non-RHD Rab36-binding proteins may also function as a Rab36 effector in certain membrane trafficking events. Further work will be necessary to identify their Rab36-binding site and their roles in Rab36-dependent membrane trafficking.

Why does Rab36 bind a variety of molecules, including the RILP family members? Because Rab36 is selectively expressed in particular cell lines, one possible answer is that Rab36 interacts with one of the Rab36-binding proteins and functions in a cell type-specific manner, as has been shown in regard to the roles of the Rab27 effector proteins Slp, Slac2, and Munc13–4 in different types of secretory cells and melanocytes (1, 39). Because RILP-L1, JIP3, and JIP4 as well
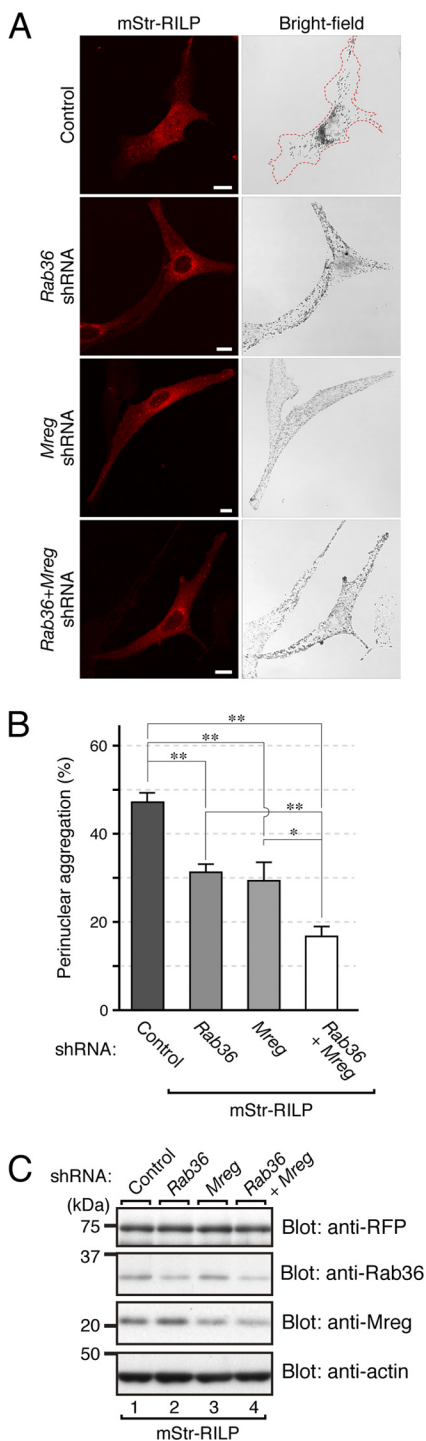
FIGURE 8. Inhibition of RILP-induced perinuclear melanosome aggregation by knockdown of Rab36 and Mreg in melanocytes. *A*, shown are typical images of RILP-expressing and Rab36-knockdown and/or Mreg-knockdown melan-a cells. Melan-a cells were transfected with *Rab36* shRNA and/or *Mreg* shRNA together with mStr-RILP. Bright-field images show the melanosome distribution. mStr-expressing cells with perinuclear melanosome aggregation are outlined with a *broken red line*. Note that simultaneous knockdown of Rab36 and Mreg by specific shRNAs suppressed the perinuclear melanosome aggregation induced by RILP much more than knockdown of either Rab36 or Mreg alone did. *Scale bars*, 10 μm. *B*, the number of melanocytes showing perinuclear melanosome aggregation is expressed as a percentage of the number of melanocytes bearing mStr fluorescence shown in *A*. *, p < 0.05; **, p < 0.01, Student's unpaired *t* test. *C*, knockdown of endogenous Rab36 protein and/or Mreg protein in melan-a cells by specific shRNAs is shown. The shRNAs and pmStr-C1-RILP were transfected into melan-a cells, and their cell lysates were subjected to 10% SDS-PAGE followed by immuno-blotting with anti-red fluorescent protein (*RFP*) antibody (1/1000 dilution; *top panel*; mStr-RILP), anti-Rab36 antibody (1 μg/ml; *second panel*), anti-Mreg antibody (0.4 μg/ml; *third panel*), and anti-actin antibody (1/10,000 dilution; *bottom panel*). The intensity of the Rab36 bands and Mreg bands on the x-ray film was captured and quantified with IMAGEJ software (Version 1.44o; NIH). After shRNA-mediated knockdown of Rab36, the band intensity was significantly reduced to 40 ± 1% (means and S.E.; *lane 2*) and 32 ± 1% (*lane 4*), in comparison with the control (*lane 1*). Similarly, after knockdown of Mreg, the band intensity was significantly reduced to 55 ± 3% (*lane 3*) and 40 ± 1% (*lane 4*), in comparison with the control (*lane 1*) (both *p* < 0.05, Student's unpaired *t* test). The blots shown are representative of three independent experiments. The residual melanosome aggregation activity of Rab36 and Mreg double knockdown melan-a cells that had been transfected with pmStr-C1-RILP may be attributable to the relatively week knockdown efficiency of *Rab36* shRNA or its low transfection efficiency. The positions of the molecular mass markers (in kilodaltons) are shown on the *left*.
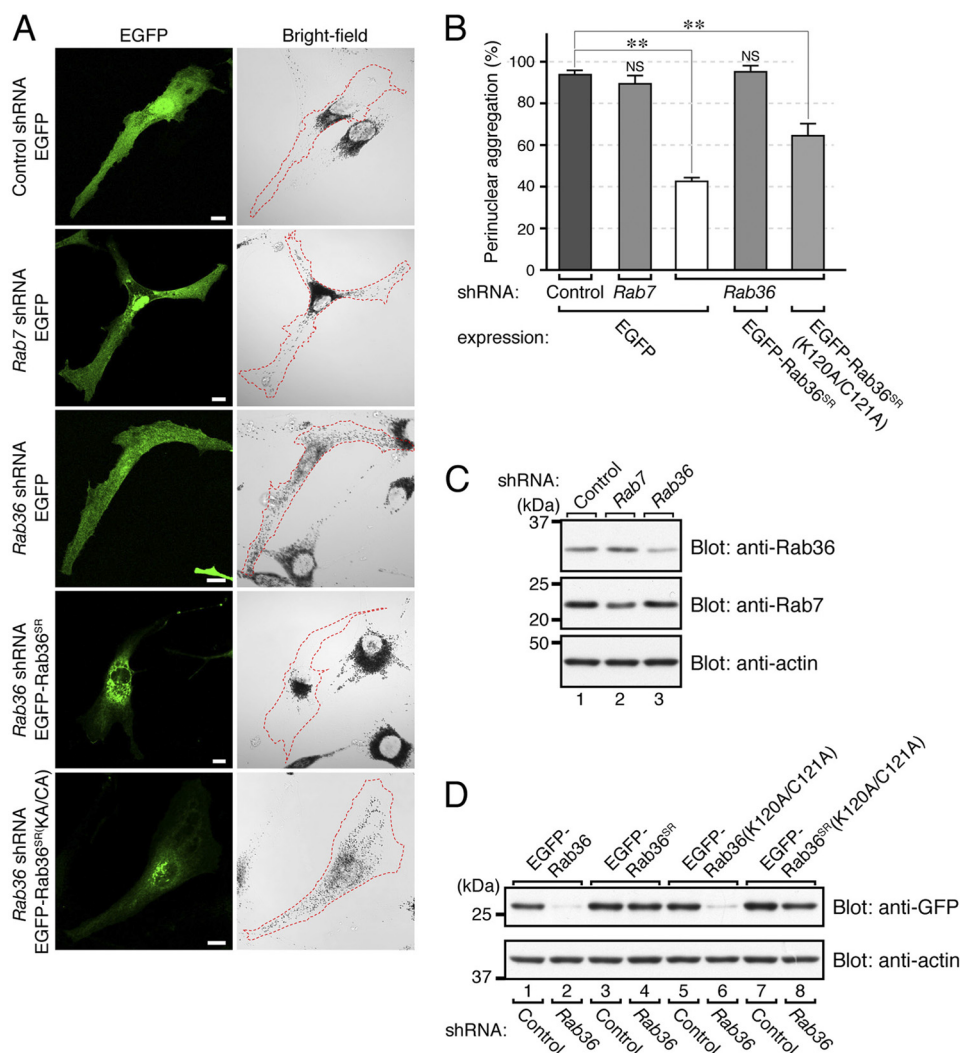
FIGURE 9. **Involvement of endogenous Rab36 protein in retrograde melanosome transport in melan-ash cells.** *A*, knockdown of endogenous Rab36 protein with a specific shRNA in melan-ash cells caused melanosomes to disperse from around the nucleus to the cell periphery. Melan-ash cells were transfected with a control shRNA, *Rab7* shRNA, or *Rab36* shRNA together with pEGFP-C1 as a transfection marker or pEGFP-C1-Rab36^{SR} (WT or K120A/C121A). Bright-field images show the melanosome distribution. EGFP-expressing cells with perinuclear melanosome aggregation are outlined with a *broken red line*. Note that knockdown of Rab36, but not of Rab7, in melan-ash cells restored the peripheral melanosome distribution and that this effect was reversed by coexpression of *Rab36* shRNA with shRNA-resistant Rab36 (Rab36^{SR}) but not with Rab36^{SR}(K120A/C121A). *Scale bars*, 10 μm. *B*, the number of melanocytes showing perinuclear melanosome aggregation is expressed as a percentage of the number of melanocytes bearing EGFP fluorescence shown in *A*. **, $p < 0.01$ in comparison with the control (Student's unpaired t test). *NS*, not significant in comparison with the control. *C*, shown is knockdown of endogenous Rab36 protein or Rab7 protein in melan-ash cells by the specific shRNA as revealed by immunoblotting with the specific antibody as described in the legend of Fig. 8*C*. *D*, an shRNA-resistant mutant of Rab36 is shown. pEGFP-C1-Rab36 (*lanes 1* and *2*), pEGFP-C1-Rab36^{SR} (*lanes 3* and *4*), pEGFP-C1-Rab36(K120A/C121A) (*lanes 5* and *6*), or pEGFP-C1-Rab36^{SR}(K120A/C121A) (*lanes 7* and *8*) was co-transfected into COS-7 cells together with pSilencer-Rab36 or a control vector. Cell lysates were subjected to 10% SDS-PAGE followed by immunoblotting with anti-GFP antibody (1/5000 dilution; *top panel*) and anti-actin antibody (1/10,000 dilution; *bottom panel*). The positions of the molecular mass markers (in kilodaltons) are shown on the *left*.

as RILP are capable of associating with a kinesin and/or dynein motor complex (40–44),[4] Rab36 may be more generally involved in the movement of Rab36-bearing vesicles/organelles in specific cell types other than melanocytes. The function of Rab36 in neurons is particularly worth investigating in the future, because Rab36 is expressed in mouse brain (Fig. 6*B*), and its absence has been proposed to be associated with epilepsy (6). Because EGFP-Rab36 is selectively targeted to the axons in hippocampal neurons and not targeted to the dendrites (45), Rab36 is presumably involved in axon-specific trafficking events, *e.g.* synaptic vesicle transport and TrkB trans-

port, both of which are mediated by a JIP3-kinesin I complex (40, 43, 44). The possible functions in neurons of Rab36 and its binding partners identified in this study are now under investigation in our laboratory.

In conclusion, we identified the RHD of RILP family members and JIP3/4 as a novel Rab36 binding domain. Although RILP was originally characterized as a Rab7 effector, our findings indicated that RILP also functions as a Rab36 effector that regulates retrograde melanosome transport in melanocytes rather than functioning as a Rab7 effector. Although the regulatory mechanism responsible for RILP using the two different Rab isoforms, Rab7 and Rab36, in different membrane trafficking events, *i.e.* in lysosome transport and in retrograde mela-

---

[4] T. Matsui and M. Fukuda, unpublished observations.

nosome transport, respectively, remains to be determined, the series of Rab binding-deficient mutants of RILP produced in this study is an ideal and powerful tool for determining which Rab functions together with RILP in particular membrane trafficking events, *e.g.* phagosome maturation (36) and lytic granule movement (37), in the future.

REFERENCES

1. Fukuda, M. (2008) Regulation of secretory vesicle traffic by Rab small GTPases. *Cell. Mol. Life Sci.* **65,** 2801–2813
2. Stenmark, H. (2009) Rab GTPases as coordinators of vesicle traffic. *Nat. Rev. Mol. Cell Biol.* **10,** 513–525
3. Hutagalung, A. H., and Novick, P. J. (2011) Role of Rab GTPases in membrane traffic and cell physiology. *Physiol. Rev.* **91,** 119–149
4. Diekmann, Y., Seixas, E., Gouw, M., Tavares-Cadete, F., Seabra, M. C., and Pereira-Leal, J. B. (2011) Thousands of rab GTPases for the cell biologist. *PLoS Comput. Biol.* **7,** e1002217
5. Mori, T., Fukuda, Y., Kuroda, H., Matsumura, T., Ota, S., Sugimoto, T., Nakamura, Y., and Inazawa, J. (1999) Cloning and characterization of a novel Rab-family gene, *Rab36*, within the region at 22q11.2 that is homozygously deleted in malignant rhabdoid tumors. *Biochem. Biophys. Res. Commun.* **254,** 594–600
6. Piccione, M., Vecchio, D., Cavani, S., Malacarne, M., Pierluigi, M., and Corsello, G. (2011) The first case of myoclonic epilepsy in a child with a de novo 22q11.2 microduplication. *Am. J. Med. Genet. A* **155,** 3054–3059
7. Chen, L., Hu, J., Yun, Y., and Wang, T. (2010) Rab36 regulates the spatial distribution of late endosomes and lysosomes through a similar mechanism to Rab34. *Mol. Membr. Biol.* **27,** 24–31
8. Fukuda, M., Kanno, E., Ishibashi, K., and Itoh, T. (2008) Large scale screening for novel Rab effectors reveals unexpected broad Rab binding specificity. *Mol. Cell Proteomics* **7,** 1031–1042
9. Kanno, E., Ishibashi, K., Kobayashi, H., Matsui, T., Ohbayashi, N., and Fukuda, M. (2010) Comprehensive screening for novel Rab-binding proteins by GST pulldown assay using 60 different mammalian Rabs. *Traffic* **11,** 491–507
10. Ohbayashi, N., Maruta, Y., Ishida, M., and Fukuda, M. (2012) Melanoregulin regulates retrograde melanosome transport through interaction with the RILP-p150[Glued] complex in melanocytes. *J. Cell Sci.* **125,** 1508–1518
11. Itoh, T., Fujita, N., Kanno, E., Yamamoto, A., Yoshimori, T., and Fukuda, M. (2008) Golgi-resident small GTPase Rab33B interacts with Atg16L and modulates autophagosome formation. *Mol. Biol. Cell* **19,** 2916–2925
12. Fukuda, M., and Mikoshiba, K. (1999) A novel alternatively spliced variant of synaptotagmin VI lacking a transmembrane domain. Implications for distinct functions of the two isoforms. *J. Biol. Chem.* **274,** 31428–31434
13. Fukuda, M., Kanno, E., and Mikoshiba, K. (1999) Conserved N-terminal cysteine motif is essential for homo- and heterodimer formation of synaptotagmins III, V, VI, and X. *J. Biol. Chem.* **274,** 31421–31427
14. Fukuda, M., Aruga, J., Niinobe, M., Aimoto, S., and Mikoshiba, K. (1994) Inositol-1,3,4,5-tetrakisphosphate binding to C2B domain of IP4BP/synaptotagmin II. *J. Biol. Chem.* **269,** 29206–29211
15. James, P., Halladay, J., and Craig, E. A. (1996) Genomic libraries and a host strain designed for highly efficient two-hybrid selection in yeast. *Genetics* **144,** 1425–1436
16. Fukuda, M. (2002) Synaptotagmin-like protein (Slp) homology domain 1 of Slac2-a/melanophilin is a critical determinant of GTP-dependent specific binding to Rab27A. *J. Biol. Chem.* **277,** 40118–40124
17. Kuroda, T. S., and Fukuda, M. (2004) Rab27A-binding protein Slp2-a is required for peripheral melanosome distribution and elongated cell shape

18. Fukuda, M. (2003) Distinct Rab binding specificity of Rim1, Rim2, rabphilin, and Noc2. Identification of a critical determinant of Rab3A/Rab27A recognition by Rim2. *J. Biol. Chem.* **278,** 15373–15380
19. Itoh, T., Satoh, M., Kanno, E., and Fukuda, M. (2006) Screening for target Rabs of TBC (Tre-2/Bub2/Cdc16) domain-containing proteins based on their Rab-binding activity. *Genes Cells* **11,** 1023–1037
20. Tsuboi, T., and Fukuda, M. (2006) Rab3A and Rab27A cooperatively regulate the docking step of dense-core vesicle exocytosis in PC12 cells. *J. Cell Sci.* **119,** 2196–2203
21. Fukuda, M., Kojima, T., Aruga, J., Niinobe, M., and Mikoshiba, K. (1995) Functional diversity of C2 domains of synaptotagmin family. Mutational analysis of inositol high polyphosphate binding domain. *J. Biol. Chem.* **270,** 26523–26527
22. Tamura, K., Ohbayashi, N., Maruta, Y., Kanno, E., Itoh, T., and Fukuda, M. (2009) Varp is a novel Rab32/38-binding protein that regulates Tyrp1 trafficking in melanocytes. *Mol. Biol. Cell* **20,** 2900–2908
23. Fukuda, M., Kobayashi, H., Ishibashi, K., and Ohbayashi, N. (2011) Genome-wide investigation of the Rab binding activity of RUN domains. Development of a novel tool that specifically traps GTP-Rab35. *Cell Struct. Funct.* **36,** 155–170
24. Bennett, D. C., Cooper, P. J., and Hart, I. R. (1987) A line of non-tumorigenic mouse melanocytes, syngeneic with the B16 melanoma and requiring a tumorpromoter for growth. *Int. J. Cancer* **39,** 414–418
25. Ali, B. R., Wasmeier, C., Lamoreux, L., Strom, M., and Seabra, M. C. (2004) Multiple regions contribute to membrane targeting of Rab GTPases. *J. Cell Sci.* **117,** 6401–6412
26. Kuroda, T. S., Ariga, H., and Fukuda, M. (2003) The actin-binding domain of Slac2-a/melanophilin is required for melanosome distribution in melanocytes. *Mol. Cell. Biol.* **23,** 5245–5255
27. Fukuda, M., and Kanno, E. (2005) Analysis of the role of Rab27 effector Slp4-a/granuphilin-a in dense-core vesicle exocytosis. *Methods Enzymol.* **403,** 445–457
28. Cantalupo, G., Alifano, P., Roberti, V., Bruni, C. B., and Bucci, C. (2001) Rab-interacting lysosomal protein (RILP). The Rab7 effector required for transport to lysosomes. *EMBO J.* **20,** 683–693
29. Wang, T., Wong, K. K., and Hong, W. (2004) A unique region of RILP distinguishes it from its related proteins in its regulation of lysosomal morphology and interaction with Rab7 and Rab34. *Mol. Biol. Cell* **15,** 815–826
30. Ostermeier, C., and Brunger, A. T. (1999) Structural basis of Rab effector specificity. Crystal structure of the small G protein Rab3A complexed with the effector domain of rabphilin-3A. *Cell* **96,** 363–374
31. Kukimoto-Niino, M., Sakamoto, A., Kanno, E., Hanawa-Suetsugu, K., Terada, T., Shirouzu, M., Fukuda, M., and Yokoyama, S. (2008) Structural basis for the exclusive specificity of Slac2-a/melanophilin for the Rab27 GTPases. *Structure* **16,** 1478–1490
32. Tamura, K., Ohbayashi, N., Ishibashi, K., and Fukuda, M. (2011) Structure-function analysis of VPS9-ankyrin-repeat protein (Varp) in the trafficking of tyrosinase-related protein 1 in melanocytes. *J. Biol. Chem.* **286,** 7507–7521
33. Fukuda, M. (2010) How can mammalian Rab small GTPases be comprehensively analyzed? Development of new tools to comprehensively analyze mammalian Rabs in membrane traffic. *Histol. Histopathol.* **25,** 1473–1480
34. Jordens, I., Fernandez-Borja, M., Marsman, M., Dusseljee, S., Janssen, L., Calafat, J., Janssen, H., Wubbolts, R., and Neefjes, J. (2001) The Rab7 effector protein RILP controls lysosomal transport by inducing the recruitment of dynein-dynactin motors. *Curr. Biol.* **11,** 1680–1685
35. Johansson, M., Rocha, N., Zwart, W., Jordens, I., Janssen, L., Kuijl, C., Olkkonen, V. M., and Neefjes, J. (2007) Activation of endosomal dynein motors by stepwise assembly of Rab7-RILP-p150[Glued], ORP1L, and the receptor βlll spectrin. *J. Cell Biol.* **176,** 459–471
36. Harrison, R. E., Bucci, C., Vieira, O. V., Schroer, T. A., and Grinstein, S. (2003) Phagosomes fuse with late endosomes and/or lysosomes by extension of membrane protrusions along microtubules. Role of Rab7 and RILP. *Mol. Cell. Biol.* **23,** 6494–6506
37. Daniele, T., Hackmann, Y., Ritter, A. T., Wenham, M., Booth, S., Bossi, G.,

Schintler, M., Auer-Grumbach, M., and Griffiths, G. M. (2011) A role for Rab7 in the movement of secretory granules in cytotoxic T lymphocytes. *Traffic* **12,** 902–911

38. O'Sullivan, T. N., Wu, X. S., Rachel, R. A., Huang, J. D., Swing, D. A., Matesic, L. E., Hammer, J. A., 3rd, Copeland, N. G., and Jenkins, N. A. (2004) *dsu* functions in a MYO5A-independent pathway to suppress the coat color of *dilute* mice. *Proc. Natl. Acad. Sci. U.S.A.* **101,** 16831–16836

39. Fukuda, M. (2005) Versatile role of Rab27 in membrane trafficking. Focus on the Rab27 effector families. *J. Biochem.* **137,** 9–16

40. Sakamoto, R., Byrd, D. T., Brown, H. M., Hisamoto, N., Matsumoto, K., and Jin, Y. (2005) The *Caenorhabditis elegans* UNC-14 RUN domain protein binds to the kinesin-1 and UNC-16 complex and regulates synaptic vesicle localization. *Mol. Biol. Cell* **16,** 483–496

41. Montagnac, G., Sibarita, J. B., Loubéry, S., Daviet, L., Romao, M., Raposo, G., and Chavrier, P. (2009) ARF6 interacts with JIP4 to control a motor switch mechanism regulating endosome traffic in cytokinesis. *Curr. Biol.* **19,** 184–195

42. Arimoto, M., Koushika, S. P., Choudhary, B. C., Li, C., Matsumoto, K., and Hisamoto, N. (2011) The *Caenorhabditis elegans* JIP3 protein UNC-16 functions as an adaptor to link kinesin-1 with cytoplasmic dynein. *J. Neurosci.* **31,** 2216–2224

43. Sun, F., Zhu, C., Dixit, R., and Cavalli, V. (2011) Sunday Driver/JIP3 binds kinesin heavy chain directly and enhances its motility. *EMBO J.* **30,** 3416–3429

44. Huang, S. H., Duan, S., Sun, T., Wang, J., Zhao, L., Geng, Z., Yan, J., Sun, H. J., and Chen, Z. Y. (2011) JIP3 mediates TrkB axonal anterograde transport and enhances BDNF signaling by directly bridging TrkB with kinesin-1. *J. Neurosci.* **31,** 10602–10614

45. Mori, Y., Matsui, T., Furutani, Y., Yoshihara, Y., and Fukuda, M. (2012) Small GTPase Rab17 regulates dendritic morphogenesis and postsynaptic development of hippocampal neurons. *J. Biol. Chem.* **287,** 8963–8973